Nanostructured Poly(vinylidene fluoride) Materials by Melt Blending with Several Percent of Acrylic Rubber

Yongjin Li,* Yuko Iwakura, Li Zhao, and Hiroshi Shimizu

Nanotechnology Research Institute, National Institute of Advanced Industrial Science and Technology (AIST), Tsukuba Central 5, 1-1-1 Higashi, Tsukuba, Ibaraki 305-8565, Japan

Received December 9, 2007; Revised Manuscript Received February 17, 2008

ABSTRACT: Nanostructured poly(vinylidene fluoride) (PVDF)/acrylic rubber (ACM) blends have been prepared by simply melt blending of PVDF and several percent of ACM. The morphology and properties of the prepared nanoblends have been investigated by means of transmission electron microscopy (TEM), dynamic mechanical analysis (DMA), differential scanning calorimetry (DSC), and polarized optical microscopy (POM). It was found that ACM has been precisely dispersed in PVDF matrix with most of the particle size of less than 100 nm. The prepared nanoblends show a unique balance between the toughness and the stiffness. The impact strength and elongation at break of the nanoblends by adding small amount of ACM increase greatly, while there is only a little decreasing in the modulus, by comparing with neat PVDF. The investigation results indicate that the nanodispersed ACM domains not only take the role of the toughening agent for PVDF but also markedly increase the crystallization speed and reduce the spherulite size of PVDF, which also contributes greatly to the enhancement of the impact strength and elongation at break.

1. Introduction

Polymer blending has been identified as the most versatile and economical method to produce new polymeric materials that are able to satisfy the complex demands for performance.[1,2] The blending to disperse one polymer (modifier) in another polymer (matrix) is typically achieved by mechanical shearing in a mixer at high temperature. The properties of prepared polymer blends are strongly dependent on the formed phase structures, e.g., size and shape of the dispersed phase. Currently, most commercial blends have a phase structure on the micrometer or submicrometer scale, so-called microstructured polymer blends. For this type of material, a large amount of modifier is usually necessary in order to achieve the desired properties. For example, to prepare a rubber-toughened plastic material, the rubber content used is usually more than 10 wt % for achieving sufficient toughening effects. Thereby, most of the investigations up to now pay most attention to the polymer blending by addition of a pretty large amount of dispersed polymer, and extensive research was conducted by adding the modifier with the interval of 10 wt % or even 20 wt %. However, the improvement of the fracture toughness of these microstructured polymer blends by addition of a large amount of rubber is inevitably accompanied by a significant drop in the modulus and tensile strength. We consider that the polymer blends with several percent of modifier in polymer matrix are also very interesting because the small amount of modifier loadings maybe leads to the very fine modifier dispersion, possible nanodispersed domains (less than 100 nm). It is expected that the inherently high surface area−volume ratio of the nanodomains plays a key role in enhancing the desired properties. On the other hand, the nanodispersed domains (impurities for the matrix) may significantly change the nature of the matrix, for example, the crystallization behavior for semicrystalline polymers or the chain entanglement density for amorphous polymers. Therefore, a nanostrutured polymer blend having an outstanding stiffness−toughness balance may be achieved. Recently, nanostructured polymer blends having a minority polymer phase with nanoscale dimensions are really attracting significant attention because they can offer many promised properties in comparison to the microstructured polymer blends.[3−10]

In this paper, we conducted the systematically investigations of the morphology and properties of poly(vinylidene fluoride) (PVDF)/acrylic rubber (ACM) blends with very minor ACM content (less than 10 wt %). It is shown that ACM was dispersed in the PVDF phase with the most of particle size of less than 100 nm, and the generated nanodomains affect the crystallization behavior and crystal morphology of the matrix PVDF significantly. The prepared nanoblends exhibit the unique stiffness−toughness balance. To our best knowledge, this is the first time to report the nanostructured polymer blend by simply blending of a matrix with several percent of commercially available modifier.

2. Experimental Section

2.1. Materials and Sample Preparation. PVDF and ACM samples used in this work were purchased from Kureha Chemicals and Nippon Zeon Co. Ltd., respectively. The molecular weight and polydispersity of the PVDF sample, determined by gel permeation chromatography, are $M_w = 209\,000$ and $M_w/M_n = 2.0$, respectively. Those for the ACM sample are $M_w = 656\,000$ and $M_w/M_n = 11.7$. All the polymers were dried in a vacuum oven at 80 °C for at least 12 h before processing. The blends with PVDF/ACM compositions varying from 99/1 to 90/10 were prepared using a Brabender plastic mixer (Toyoseiki Co. KF70V) with a twin screw at a screw rotation speed of 100 rpm at 190 °C for 10 min. After blending, all the samples were then hot pressed at 200 °C to a film with a thickness of 500 μm, followed by quenching in ice–water. The obtained films were used for the following characterization.

2.2. Structural Characterization. Phase structure of the blends was observed directly using a transmission electron microscope (TEM) (Hitachi H7000) operating at an acceleration voltage of 75 kV. The blend samples were ultramicrotomed at −120 °C to a section with a thickness of about 70 nm. The sections were then stained by ruthenium tetroxide (RuO_4) for 20 min.

Dynamic mechanical analysis (DMA) was carried out with RHEOVIBRON DDV-25FP (Orientec Corp.) in a tensile mode. The dynamic storage and loss moduli were determined at a frequency of 1 Hz and a heating rate of 3 °C/min as a function of temperature from −150 to 170 °C.

Differential scanning calorimetry (DSC) was carried out under nitrogen flow at a heating or cooling rate of 10 K/min with a Perkin-

* To whom correspondence should be addressed. E-mail: yongjin-li@aist.go.jp.

10.1021/ma7027402 CCC: $40.75
Published on Web 04/08/2008

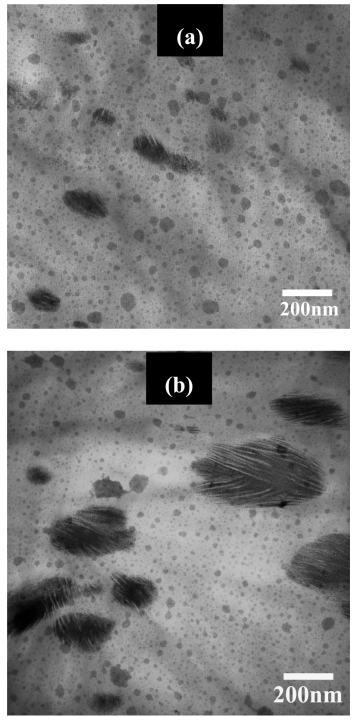

Figure 1. Transmission electron micrographs for (a) PVDF/ACM = 97/3 and (b) PVDF/ACM = 90/10.

Elmer DSC-7 differential scanning calorimeter calibrated with the melting temperature of indium and zinc. All the DSC curves were normalized by sample weight after a baseline correction.

A polarized optical micrograph (POM) was obtained under crossed polarizers using an Olympus BX51. The hot pressed blend samples were microtomed at room temperature to a section with a thickness of about 10 μm. The sections were directly used for POM observation.

2.3. Physical Property Measurements. A tensile test was carried out according to the ASTM D 412-80 test method using dumbbell-shaped samples punched out from the molded sheets. The tests were performed using a tensile testing machine, Tensilon UMT-300 (Orientec Co., Ltd.), at a crosshead speed of 10 mm/min at 20 °C and 50% relative humidity. Three specimens were tested for each sample.

Film impact tests were carried out according to JIS K7160 procedures using a standard impact tester (Toyoseiki Co. Ltd., Japan) at 20 °C and 50% relative humidity. At least five specimens were tested for each sample to get an average value.

3. Results

3.1. Nanodispersion of ACM in PVDF Matrix. Figure 1 shows the TEM images for the PVDF/ACM blends with 3 and 10 wt % ACM. In this figure, PVDF is observed as a white phase and ACM is observed as a dark phase because ACM is more readily stained than PVDF. It can be seen that numerous of ACM domains are precisely dispersed in the PVDF phase with the domain size varying from 10 to 100 nm for the PVDF/ACM = 97/3 blends (Figure 1a). Although many researchers have successfully prepared nanoblends using block copolymers,[4,5,9–12] reactive blending,[3,6] or high-shear processing,[7,8] to our knowledge, this is the first time to report the homogeneously nanodispersed polymer blend by simply blending of two commercial polymers. With increasing the ACM content, the domain size distribution increases. As shown in Figure 1b, some ACM domains with the size of 100−200 nm are observed in addition to the ACM nanodomains. It is considered that the large ACM domains seriously deteriorate the modulus of the prepared polymer blend. Therefore, we will concentrate our investigations on the blends with the ACM additions of less than 10 wt %.

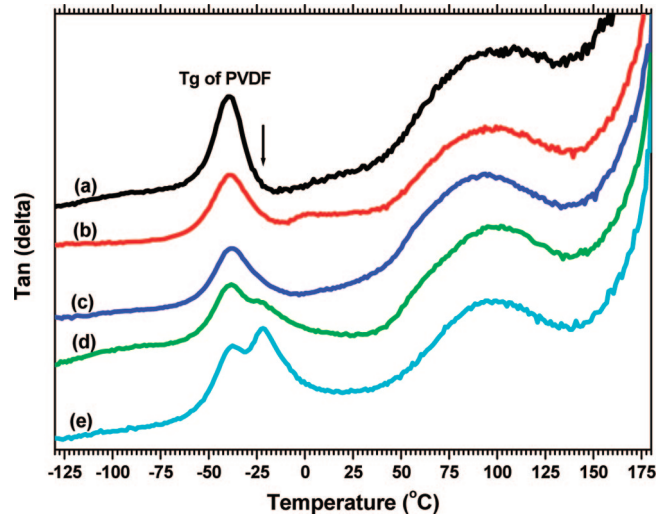

Figure 2. Tan(δ) as a function of temperature for (a) neat PVDF, (b) PVDF/ACM = 99/1, (c) PVDF/ACM = 97/3, (d) PVDF/ACM = 95/5, and (e) PVDF/ACM = 90/10.

3.2. Dynamical Mechanical Analysis. Figure 2 shows plots of the dynamic loss (tan δ) by DMA as a function of temperature for neat PVDF and PVDF/ACM nanoblends. Neat PVDF shows a very sharp relaxation peak at –40 °C. The relaxation is assigned to the motion of the main chain in amorphous region; thus, the peak temperature is regarded as the glass transition temperature of PVDF.[13] The relaxation peak becomes wider with addition of 1 and 3 wt % ACM in the PVDF, as compared with the peak of neat PVDF. The broadening of the relaxation peak may be due to the PVDF geometrically constrained at the interface between the PVDF matrix and the ACM nanodomains. For the PVDF/ACM = 95/5 blend, a shoulder is observed at the temperature of –24 °C. The shoulder corresponds to the relaxation of ACM molecular chains. The PVDF/ACM = 90/10 blend shows a very clear ACM relaxation peak at –20 °C, except for the glass transition of PVDF. The fact that two relaxation peaks are observed for the blends with large ACM inclusions indicates the phase-separated morphology, which is consistent with the TEM results in Figure 1. On the other hand, the T_g of neat ACM has been reported to be –12.8 °C.[14] The large shift of the ACM relaxation peak suggests that the ACM phase in the nanoblends contains a considerable fraction of PVDF.

3.3. Thermal Behaviors of the Nanoblends. Figure 3 shows the DSC cooling curves for neat PVDF and the PVDF/ACM nanoblends from the melt state. The thermal history of the all samples is diminished by keeping the samples at 230 °C for 5 min because the temperature is much higher than the equilibrium melting temperature of PVDF.[15] At least two main features for this nonisothermal crystallization behavior of the nanoblends can be noted by comparison to neat PVDF. First, the crystallization peak temperature shifts to higher temperature region upon adding small amount of ACM, as shown in Figure 4. The increased crystallization temperature in the nanoblends indicates that PVDF has a higher crystallization rate in the nanoblends than in neat PVDF. The crystallization peak temperature takes the maximum shifts upon adding 3 wt % ACM. Further increasing the ACM content in the blend results in shifting of the crystallization peak to a lower temperature. For the PVDF/ACM = 80/20 blend, the crystallization peak temperature is 135 °C, which is lower than 138 °C for neat PVDF. The results demonstrate that large ACM inclusion decreases the crystal-

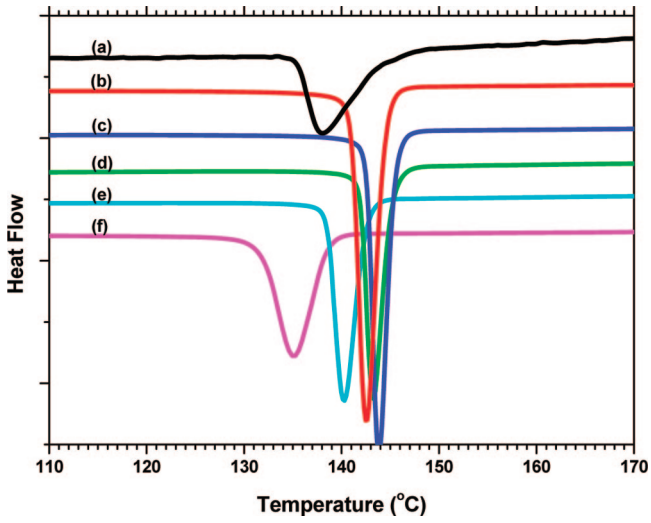

Figure 3. DSC thermograms during cooling from melt for neat PVDF and PVDF/ACM blends: (a) neat PVDF, (b) PVDF/ACM = 99/1, (c) PVDF/ACM = 97/3, (d) PVDF/ACM = 95/5, (e) PVDF/ACM = 90/10, and (f) PVDF/ACM = 80/20.

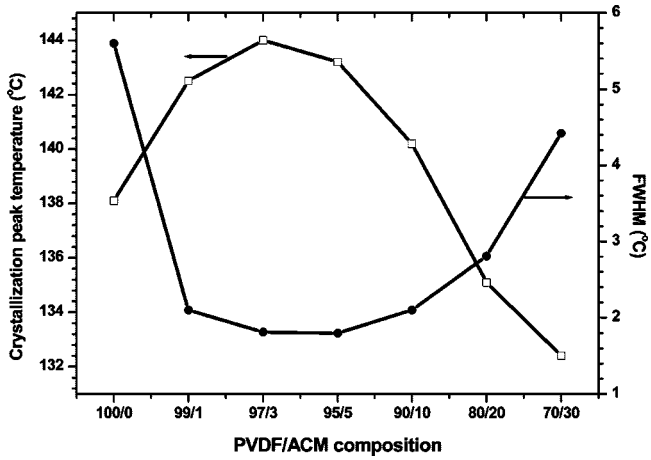

Figure 4. Nonisothermal crystallization peak temperature and full width at half-maximum (fwhm) of the endothermic peak for neat PVDF and PVDF/ACM blends.

lization rate. Second, it is clear from the figure that crystallization peak of the nanoblends is more symmetric and sharper than that of neat PVDF. Figure 4 shows the crystallization peak temperature and full width at half-maximum (fwhm) of endothermic peak as a function of the ACM content in the blends. The fwhm value abruptly decreases from 5.6 to 2.1 °C upon addition of only 1 wt % ACM. It keeps almost constant up to the 10 wt % addition of ACM and then increases with the ACM content. The decreased fwhm of the exothermic peak indicates the narrower time distributions for the nucleation and growth of the formed PVDF crystals in the nanoblends. The nonisothermal crystallization behavior of the PVDF/ACM blend suggests that the nanodispersed ACM domains act as the nuclei for PVDF crystallization from melt state, while the ACM big domains in the submicrometer scale impede the growth of PVDF crystals.

Figure 5 shows the DSC heating thermograms of the neat PVDF and the PVDF/ACM nanoblends. No clear melting temperature change for PVDF was found upon the addition of small amount of ACM, but the melting peaks for the nanoblend are sharper than that for the neat PVDF. Note that the PVDF crystallinity keeps almost constant (about 49.5%) based on the

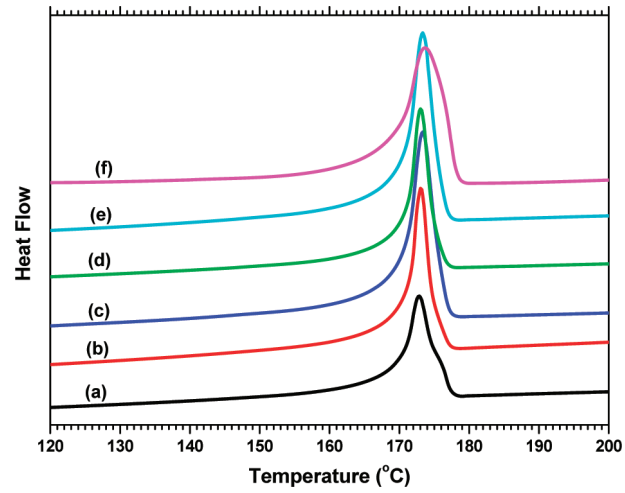

Figure 5. DSC thermograms during heating for neat PVDF and PVDF/ACM blends: (a) neat PVDF, (b) PVDF/ACM = 99/1, (c) PVDF/ACM = 97/3, (d) PVDF/ACM = 95/5, (e) PVDF/ACM = 90/10, and (f) PVDF/ACM = 80/20.

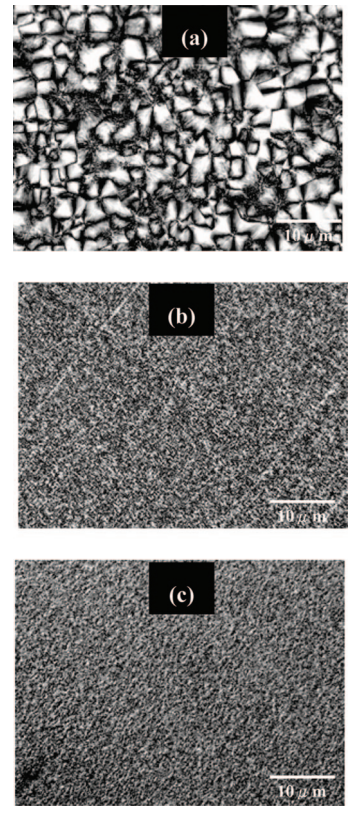

Figure 6. Polarized optical microscopy images for (a) neat PVDF, (b) PVDF/ACM = 99/1, and (c) PVDF/ACM = 90/10.

area of exothermic peak during heating for the PVDF/ACM nanoblend and neat PVDF.

3.4. Crystal Morphologies in Neat PVDF and in the Nanoblends. The polarized optical microphotographs for neat PVDF and the PVDF/ACM nanoblends are shown in Figure 6. It should be noted that the slices used for POM measurements were directly microtomed from the melt-blended samples. It can be seen that the neat PVDF forms distinct crystalline spherulites with the size of more than 10 μm. The presence of ACM nanodomains drastically reduces the spherulites size as evident from the Figure 6b, where the blend contains only 1 wt

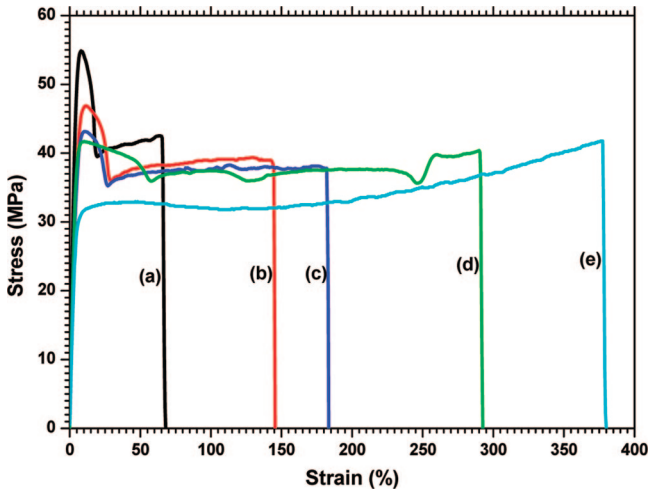

Figure 7. Strain−stress curves for (a) neat PVDF, (b) PVDF/ACM = 99/1, (c) PVDF/ACM = 97/3, (d) PVDF/ACM = 95/5, and (e) PVDF/ACM = 90/10.

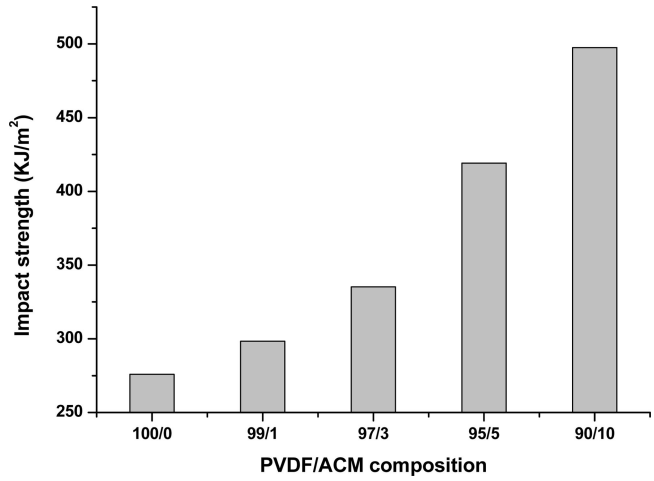

Figure 8. Film impact strength for neat PVDF and the PVDF/ACM nanoblends.

% ACM. No significant difference in the spherulite size was observed by further increasing the ACM content in the blend, as seen in Figure 6c.

3.5. Mechanical Properties of the Nanoblends. Strain−stress curves of neat PVDF and the PVDF/ACM nanoblends are shown in Figure 7. The neat PVDF is very rigid and undergoes very clear yielding (necking) upon increasing the tensile strain. It breaks at the elongation of about 65% with the further increasing the strain. However, it is found that the necking process occurs at larger strain for the nanoblend with addition of only 1 wt % ACM in PVDF compared to the neat PVDF. The blend undergoes considerable cold drawing after the yielding and then breaks at the strain of 145%, which is a significant increase in the elongation at break by adding only 1 wt % ACM. The necking phenomenon in the nanoblends is suppressed with increasing ACM content, and the ductility is consequently improved. For the nanoblend with 10 wt % ACM, no yielding behavior is observed, and the sample is homogeneously elongated upon applying the tensile stress. The elongation at break of this blend is 380%, which is about 6 times that of the neat PVDF.

The film impact strength of neat PVDF and the PVDF/ACM nanoblends is shown in Figure 8. Significant improvement can be observed even with the addition of only 1 wt % ACM. The toughness increases with increasing the ACM content. The impact strength for the PVDF/ACM = 90/10 blend is as high as 502 J/ m^2, which is about 100% higher than the value for neat PVDF.

It should be noted that the addition of several percent of ACM shows less effect on the tensile strength and the modulus of PVDF, as the modified PVDF maintains quite high tensile modulus and tensile strength. The tensile strength at break for the PVDF/ACM = 90/10 blends is 43.7 MPa, which is even higher than that for the neat PVDF, 43.1 MPa. The results are very significant in obtaining a material having remarkable stiffness−toughness balance.

4. Discussion

4.1. Formation of Nanoblends by the Simply Melt-Blending. Here we show a very simple method to prepare nanostructured polymer blends, and this concept may be applied more generally to other polymer materials. However, it is considered that the miscibility and the composition ratio between the used polymers are important for fabricating this type of nanoblend. The blending of two thermodynamic miscible polymers leads to the molecular chain mixings, and no phase separation occurs. In contrast, only the microstructured polymer blend can be obtained if the totally immiscible polymer pairs are used even with the very small amount of modifier addition. We consider that the appropriate miscibility not only induces the heterogeneous (phase-separated) structures but also gives guarantees of the precise dispersion of modifier, which is prerequisite for the formation of this type of nanoblends. There is a very good compatibility between PVDF and ACM, which can be attributed to the dipolar interaction between CF_2 groups in PVDF and ester groups in ACM. PVDF and poly(methyl methacrylate) (PMMA) are really a thermodynamic miscible polymer pair.[16–18] However, the interaction between PVDF and ACM is weaker than that between PVDF and PMMA due to the lower carbonyl group concentration in the ACM copolymer. Therefore, PVDF forms a partially miscible polymer blend with ACM in the composition ratios investigated here. One can speculate that, at low ACM content, the blend is totally homogeneous at the blending temperature under the mechanical shearing for this partially miscible blend. The spinodal decomposition takes place upon cooling from the mixing temperature, and phase separation occurs. The size of the appearing inhomogeneities varies with the solidification process of the blends.[19–22] For the blends with very low ACM contents (<10 wt %), the phase separates at a temperature not far from the PVDF crystallization temperature, and ACM forms numerous domains with the size of less than 100 nm. Therefore, a nanoblend was obtained. The mechanism is supported by the DMA results in Figure 2. The shift of T_g of ACM in nanoblends with respect of the neat ACM T_g indicates the ACM phase contains some PVDF due to the incomplete phase separation by spinodal decomposition. For the blends with large ACM contents, either the PVDF/ACM mixture is still phase-separated at the blending temperature or the spinodal decomposition takes place at a temperature sufficiently high with respect to the crystallization temperature, and the coalescence and Oswald ripening occur before the crystallization of PVDF. In both cases, ACM formed the domains with the size in micrometer scale. Our observation for the PVDF/ACM = 80/20 blends shows that almost all the ACM domains are really in submicrometer scale.

4.2. Effects of Nanodomains on the Properties of the Blend Material. Toughening of semicrystalline polymers by blending with elastomers has been extensively reported. Significant efforts have been made to tailor the morphology of the dispersed elastomer phase, and it is well established that the particle size plays a crucial role in governing the level of

toughening.[23–26] It was shown that the particles over several microns in diameter are often too large to interact with the stress field at the crack tip, while the rubber particle under 100 nm appear to be too small to cavitate effectively. However, we here found that the ACM nanodomains with the domains size of less than 100 nm in PVDF matrix shows markedly increased elongation at break and impact strength as well. It is obvious that the widely used cavitation toughening mechanism cannot be applied for the present system. We attributed the toughening effects to two factors induced by the dispersed nanodomains. First, the very small rubber interparticle distance in the nanoblends may lead to the plastic deformation of the matrix upon the impact and the process dissipates a lot of energy.[27,28] Second, the numerous ACM nanodomains show dramatic effects on the original properties of PVDF matrix. The mechanical properties of the blends can be therefore changed. The DSC results show that an increase of 5.5 °C in the crystallization temperature is achieved with the addition of 3 wt % ACM, implying that the ACM nanodomains are a very effective nucleating agent for the PVDF matrix. If some of these nanodomains become the nucleating sites, then the number of spherulites will increase dramatically and the size of the spherulites will reduce significantly. This is the real fact observed from Figure 6. Numerous investigations have been made on the spherulites size effects on the mechanical and fracture properties of semicrystalline polymers.[29–31] Strong evidence showed that the semicrystalline polymer with small spherulites tends to be tougher than the one with coarse spherulites because larger spherulites have weaker boundaries. In addition, a decrease in the spherulite size suppresses the necking (yielding) behavior of a crystalline polymer because the necking point for the semicrystalline polymers is believed to relate to the break of a large crystal spherulite upon the tensile deformation.

On the other hand, the crystallinity of PVDF keeps almost constant upon the addition of small amount of ACM, which is thought to be beneficial for keeping the high modulus and tensile strength of the nanoblends.

5. Conclusion

We report that a nanostructured PVDF blend was created by simply melt mixing of PVDF with several percent of ACM. The generation of ACM nanodomains in the PVDF matrix improved the toughness and elongation at break significantly as compared to unmodified PVDF, while the nanoblend maintained a pretty high strength and modulus values. The investigation indicated that the ACM nanodomains accelerate the PVDF crystallization and reduce the size of PVDF spherulites in the blend, which takes a critical role for the improvement of the ductility of the fabricated nanoblends. The work provides a new route to fabricate nanostructured polymer blend, and the preparation strategy should also be applicable to some other polymer blend systems.

Acknowledgment. This work is supported by the New Energy and Industrial Technology Development Organization (NEDO) for the "Project on the Nanostructured Polymeric Materials". The useful discussion with Prof. Takashi Inoue from Yamagada University is greatly appreciated. The authors thank the reviewers for valuable suggestions.

References and Notes

(1) Utracki, L. A. *Polymer Alloys and Blends*; Hanser: New York, 1989.
(2) Paul, D. R.; Newman, S. *Polymer Blend*; Academic Press: New York, 1978; Vol 1.
(3) Pernot, H.; Baumert, M.; Court, F.; Leibler, L. *Nat. Mater.* **2002**, *1*, 54–58.
(4) Koulic, C.; Jerome, R. *Macromolecules* **2004**, *37*, 888–893.
(5) Koulic, C.; Jerome, R. *Macromolecules* **2004**, *37*, 3459–3469.
(6) Hu, G. H.; Cartuer, H.; Plummer, C. *Macromolecules* **1999**, *32*, 4713–4718.
(7) Shimizu, H.; Li, Y.; Kaito, A.; Sano, H. *Macromolecules* **2005**, *38*, 7880–7883.
(8) Li, Y.; Shimizu, H.; Furumichi, T.; Takahashi, Y.; Furukawa, T. *J. Polym. Sci., Polym. Phys.* **2007**, *45*, 2707–2714.
(9) Ritzenthaler, S.; Court, F.; David, L.; Girard-Reydet, E.; Leibler, L.; Pascault, J.-P. *Macromolecules* **2002**, *35*, 6245–6254.
(10) Bhardwaj, R.; Mohanty, A. K. *Biomacromolecules* **2007**, *8*, 2476–2484.
(11) Ruzette, A. V.; Leibler, L. *Nat. Mater.* **2005**, *4*, 19–31.
(12) Leibler, L. *Prog. Polym. Sci.* **2005**, *30.*, 898–914.
(13) Imken, R. L.; Paul, D. R.; Barlow, J. W. *Polym. Eng. Sci.* **1976**, *9*, 593–602.
(14) Li, Y.; Oono, Y.; Nakayama, K.; Shimizu, H.; Inoue, T. *Polymer* **2006**, *47*, 3946–3953.
(15) Takahashi, Y.; Tadokoro, H. *Macromolecules* **1980**, *13*, 1317–1320.
(16) Penning, J. P.; Manley, R. St. J. *Macromolecules* **1996**, *29*, 77–83.
(17) Rahman, M. H.; Nandi, A. K. *Macromol. Chem. Phys.* **2002**, *203*, 653–662.
(18) Bernstein, R. E.; Paul, D. R.; Barlow, J. W. *Polym. Eng. Sci.* **1978**, *18*, 1225–1232.
(19) De Gennes, P. G. *J. Chem. Phys.* **1980**, *72*, 4756–4763.
(20) Binder, K.; Frisch, H. L. *Macromolecules* **1984**, *17*, 2928–2930.
(21) Jilge, W.; Carnesin, I.; Kremer, K.; Binder, K. *Macromolecules* **1990**, *23*, 5001–5013.
(22) Sano, H.; Yui, H.; Li, H.; Inoue, T. *Polymer* **1998**, *39*, 5265–5267.
(23) Wu, S. *Polymer* **1985**, *26*, 1855–1863.
(24) Bartczak, Z.; Argon, A. S.; Cohen, R. E.; Weinberg, M. *Polymer* **1999**, *40*, 2331–2346.
(25) Muratoglu, O. K.; Argon, A. S.; Cohen, R. E.; Weinberg, M. *Polymer* **1995**, *36*, 921–930.
(26) Kayano, Y.; Keskkula, H.; Paul, D. R. *Polymer* **1998**, *39*, 2835–2845.
(27) Wu, S. *Polymer* **1985**, *26*, 1855–1863.
(28) Van der Sanden, M. C. M.; Meijer, H. E. H.; Lemstra, P. J. *Polymer* **1993**, *34*, 2148–2154.
(29) Friedrich, K. *Adv. Polym. Sci.* **1983**, *52/53*, 225–308.
(30) Magenity, P. M.; Hooper, J. J.; Payneter, C. D.; Riley, A. M.; Nutbeem, C.; Elton, N. J.; Adams, J. M. *Polymer* **1992**, *24*, 5215–5224.
(31) Oliveira, M. J.; Cramez, M. C. *J. Macromol. Sci., Phys.* **2001**, *B40*, 457–471.

MA7027402